2008 *Biochemistry* **2010,** *49,* 2008–2017
DOI: 10.1021/bi901851y

BIOCHEMISTRY
including biophysical chemistry & molecular biology
Article

Kinetic Mechanistic Studies of Wild-Type Leucine-Rich Repeat Kinase2: Characterization of the Kinase and GTPase Activities

Min Liu,*[,‡] Brittany Dobson,[‡] Marcie A. Glicksman,[‡] Zhenyu Yue,[§] and Ross L. Stein[∥]

[‡]*Laboratory for Drug Discovery in Neurodegeneration, Harvard NeuroDiscovery Center, 65 Landsdowne Street, Fourth Floor, Cambridge, Massachusetts 02139,* [§]*Department of Neurology, Mount Sinai School of Medicine, New York, New York 10029-6500, and* [∥]*Discovery Research, Sirtris Pharmaceuticals, Cambridge, Massachusetts 02139*

Received October 28, 2009; Revised Manuscript Received January 13, 2010

ABSTRACT: Recent studies have identified mutations in the leucine-rich repeat kinase2 gene (LRRK2) in the most common familial forms and some sporadic forms of Parkinson's disease (PD). LRRK2 is a large and complex protein that possesses kinase and GTPase activities. Some LRRK2 mutants enhance kinase activity and possibly contribute to PD through a toxic gain-of-function mechanism. Given the role of LRRK2 in the pathogenesis of PD, understanding the kinetic mechanism of its two enzymatic properties is critical for the discovery of inhibitors of LRRK2 kinase that would be therapeutically useful in treating PD. In this report, by using LRRK2 protein purified from murine brain, first we characterize kinetic mechanisms for the LRRK2-catalyzed phosphorylation of two peptide substrates: PLK-derived peptide (PLK-peptide) and LRRKtide. We found that LRRK2 follows a rapid equilibrium random mechanism for the phosphorylation of PLK-peptide with either ATP or PLK-peptide being the first substrate binding to the enzyme, as evidenced by initial velocity and inhibition mechanism studies with nucleotide analogues AMP and AMP-PNP, product ADP, and an analogue of the peptide substrate. The binding of the first substrate has no effect on the binding affinity of the second substrate. Identical mechanistic conclusions were drawn when LRRKtide was the phosphoryl acceptor. Next, we characterize the GTPase activity of LRRK2 with a k_{cat} of $0.2 \pm 0.02\ s^{-1}$ and a K_m of $210 \pm 29\ \mu M$. A SKIE of 0.97 ± 0.04 was measured on k_{cat} for the GTPase activity of LRRK2 in a D_2O molar fraction of 0.86 and suggested that the product dissociation step is rate-limiting, of the steps governed by k_{cat} in the LRRK2-catalyzed GTP hydrolysis. Surprisingly, binding of GTP, GDP, or GMP has no effect on kinase activity, although GMP and GDP inhibit the GTPase activity. Finally, we have identified compound LDN-73794 through screen of LRRK2 kinase inhibitors. Our study revealed that this compound is a competitive inhibitor of the binding of ATP and inhibits the kinase activity without affecting the GTPase activity.

Parkinson's disease, characterized by tremor, rigidity, bradykinesia, and postural instability, is the second most common neurodegenerative disorder. It affects more than 1 million Americans, and more than 60000 patients are newly diagnosed each year. PD[1] is caused by the loss of dopaminergic neurons in the *substantia nigra*. Normally, these neurons produce dopamine, an essential chemical messenger in the brain. Once damaged, these neurons stop producing dopamine and compromise the brain's ability to control movement. Mutations in several genes have been genetically linked to PD in recent years (*1*). Among those genes, leucine-rich repeat kinase2 (LRRK2) has emerged as the most relevant player in PD pathogenesis. At least 20 mutations in LRRK2 have been found in the most common familial forms and some sporadic forms of PD (*2*−*6*).

LRRK2 is a large and complex protein containing several independent domains, including a leucine-rich repeat (LRR) domain, a Roc domain followed by its associated COR domain, a kinase domain, and a C-terminal WD40 domain (*7*, *8*). LRRK2 is unusual in that it encodes two distinct but functionally linked enzymes: a protein kinase and a GTPase. Recent studies have suggested that LRRK2 is capable of undergoing both autophosphorylation and generic substrate phosphorylation, and the kinase activity is regulated by the GTPase domain (*8*−*12*). The elevated kinase activity found in some PD-associated mutations results in neuronal cell death, whereas kinase-dead variants of LRRK2 protect neuronal cells from death (*8*, *13*, *14*). Clearly, kinase activity is a critical component of LRRK2 function.

Since the emerging evidence implicates LRRK2 kinase activity in the pathogenesis of PD, identifying inhibitors of LRRK2 kinase has become a priority in the validation of kinase activity as a drug target and the search for drugs to treat PD. A detailed understanding of the kinetic mechanism underlying the two enzymatic properties of LRRK2 (kinase and GTPase) is critical for the discovery and design of inhibitors. However, such information is quite limited. As part of a program to find inhibitors of LRRK2 kinase, we conducted kinetic mechanistic studies with wild-type full-length LRRK2. Specifically, we report results of studies that aimed (i) to understand the kinetic mechanism of LRRK2-catalyzed phosphorylation of two peptide substrates (PLK-peptide and LRRKtide), (ii) to characterize the

*To whom correspondence should be addressed: Laboratory for Drug Discovery in Neurodegeneration, Harvard NeuroDiscovery Center, 65 Landsdowne St., Fourth Floor, Cambridge, MA 02139. Phone: (617) 768-8658. Fax: (617) 768-8606. E-mail: mliu@rics.bwh.harvard.edu.

[1]Abbreviations: PD, Parkinson's disease; wt LRRK2, wild-type leucine-rich repeat kinase2; PLK-peptide, PLK-derived peptide with a motif of RRRSLLE; LRRKtide, RLGRDKYKTLRQIRQ; LRRKtide[A], RLGRDKYKALRQIRQ.

 Published on Web 02/10/2010

GTPase activity, (iii) to elucidate the functional relationship between GTPase activity and kinase activity, i.e., how the kinase activity is regulated, and (iv) to investigate the mechanism of inhibition of a compound identified through a screen.

MATERIALS AND METHODS

Materials. ATP, ADP, AMP, GDP, GMP, DTT, magnesium chloride, HEPES, and bovine serum albumin were purchased from Sigma (St. Louis, MO). GTP was from Bioline (Taunton, MA). Peptides LRRKtide (RLGRDKYKTLRQIRQ) and LRRKtide^{A} (RLGRDKYKALRQIRQ) were purchased from American Peptide (Sunnyvale, CA). PLK-peptide (PLK-derived peptide with a motif of RRRSLLE), Eu-antiphospho-PLK, [γ-^{33}P]ATP, [α-^{14}C]ADP, and [α-^{33}P]GTP were from Perkin-Elmer (Boston, MA). LRRK2 was purified from BAC-transgenic mouse brain as described by Li (*15*).

TR-FRET Assay of LRRK2-Catalyzed PLK-peptide Phosphorylation. The kinase assay for phosphorylation of PLK-peptide (motif of RRRSLLE) was conducted in buffer containing 20 mM HEPES (pH 7.4), 50 mM NaCl, 10 mM $MgCl_2$, 1 mM DTT, 0.5 mg/mL BSA, 1 mM β-Gly-PO_4, PLK-peptide, and ATP. β-Gly-PO_4 is a phosphatase inhibitor and is added to protect against phosphatases. PLK-peptide and ATP were used at various concentrations as indicated in the Results. The reactions were conducted in duplicate and initiated by the addition of 4 nM LRRK2, and the mixtures were incubated at room temperature for 4 h. The reaction was stopped by the addition of 10 mM EDTA and the mixture incubated with 2 nM Eu-antiphospho-PLK for 2 h. The TR-FRET signal was read with an EnVision plate reader (PerkinElmer). In all cases, reaction progress curves for production of phospho-PLK-peptide were linear over at last 6 h and allowed calculation of initial velocities.

Kinetic Analysis of LRRK2-Catalyzed LRRKtide Phosphorylation. The kinase assay for phosphorylation of LRRKtide (RLGRDKYKTLRQIRQ) was conducted in buffer containing 20 mM HEPES (pH 7.4), 50 mM NaCl, 10 mM $MgCl_2$, 1 mM DTT, 0.5 mg/mL BSA, 1 mM β-Gly-PO_4, LRRKtide, ATP, and [γ-^{33}P]ATP. LRRKtide and ATP were used at various concentrations as indicated in the Results, and the ratio of ATP to [γ-^{33}P]ATP was kept constant at all ATP concentrations (250 μM ATP and 5 μCi of [γ-^{33}P]ATP). The reactions were conducted in duplicate and initiated by the addition of 100 nM LRRK2, and the mixtures were incubated at room temperature for 45 min. The reaction was stopped by the addition of 20 mM EDTA, and the mixture was transferred to a multiscreen PH filtration plate (Millipore, Billerica, MA) and washed six times with 75 mM H_3PO_4. The plate was dried; filters were removed, and the samples were counted with a scintillation counter. Background reaction was conducted in the absence of LRRK2. In all cases, reaction progress curves for production of phospho-LRRKtide were linear over at last 60 min and allowed calculation of initial velocities.

Kinetic Analysis of LRRK2-Catalyzed GTP Hydrolysis. The GTPase assay was conducted in buffer containing 20 mM Tris (pH 7.4), 50 mM NaCl, 10 mM $MgCl_2$, 1 mM DTT, 0.5 mg/mL BSA, GTP, and [α-^{33}P]GTP. The reactions were conducted in triplicate and initiated by the addition of 30 nM LRRK2, and the mixtures were incubated at room temperature for 20 min. The reaction was stopped by the addition of 20 mM EDTA, and the product [α-^{33}P]GDP was separated from [α-^{33}P]GTP by PEI-cellulose thin layer chromatography (TLC) (Sigma) developed with 0.5 M KH_2PO_4 (pH 3.4) developing buffer and analyzed with a scintillation counter. In all cases, reaction progress curves for GTP hydrolysis were linear over at last 30 min and allowed calculation of initial velocities.

Data Analysis via Basic Equations. Data were analyzed by nonlinear least-squares, using either Sigma-Plot or Grafit. Standard kinetic mechanisms for two-substrate reactions and their rate equations are shown below.

Ping-pong:

$$v = \frac{k_{cat}[E][A][B]}{K_A[B] + K_B[A] + [A][B]} \quad (1)$$

where K_A and K_B are Michaelis constants.

Rapid equilibrium ordered:

$$v = \frac{k_{cat}[E][A][B]}{K_A K_B + K_B[A] + [A][B]} \quad (2)$$

where K_A and K_B are substrate dissociation constants for the EA and EB complexes, respectively.

Rapid equilibrium random/steady-state ordered:

$$v = \frac{k_{cat}[E][A][B]}{\alpha K_A K_B + \alpha K_A[B] + \alpha K_B[A] + [A][B]} \quad (3)$$

For rapid equilibrium systems, K_A, K_B, αK_A, and αK_B are substrate dissociation constants for the EA, EB, and EAB complexes; for steady-state systems, K_A is substrate dissociation constant for the EA complex. αK_A and αK_B are Michaelis constants. See ref *16* for definitions of mechanisms, substrate dissociation constants, and α.

RESULTS

Evaluation of the TR-FRET Assay. We chose PLK-peptide (based around the putative phosphorylation site of PLK protein) as the phosphoryl acceptor and developed a sensitive TR-FRET assay. To evaluate this assay, we ran a radiometric assay under the same conditions. The initial velocities were measured as a function of PLK-peptide concentration at 200 μM ATP and 24 nM LRRK2 in both assays (Figure 1). Similar kinetics were obtained from the two assays; both data sets adhered to the simple Michaelis−Menten equation, yielding steady-state kinetic parameter estimates: $(k_{cat})_{app}$ = 31870 ± 837 FU/h and $(K_{PLK})_{app}$ = 592 ± 56 nM for the TR-FRET assay, and $(k_{cat})_{app}$ = 33.6 ± 3.5 nM/h and $(K_{PLK})_{app}$ = 434 ± 16 nM for the radiometric assay. Linear correlation between the FU/h unit and the nM/h unit allows us to calculate a proportionality factor of 855 ± 108 FU/nM that can be used to convert initial velocities from units of FU/h to units of nM/h.

Initial Velocity Studies of the LRRK2-Catalyzed Phosphorylation of PLK-peptide. To determine the kinetic mechanism for the LRRK2-catalyzed phosphorylation of PLK-peptide, initial velocities were measured as a function of PLK-peptide concentration, at several fixed concentrations of ATP (Figure 2A). The complete data set was subjected to global analysis by nonlinear least-squares fits to the three standard mechanisms, using eqs 1−3. Statistically, the random mechanism (or steady-state ordered mechanism) fits the data the best and gives the following estimates averaged from two independent experiments: k_{cat} = 0.024 ± 0.002 min^{-1}, K_{ATP} = 13 ± 3 μM, K_{PLK} = 0.58 ± 0.1 μM, and α = 1.3 ± 0.2 (summarized in Table 1).

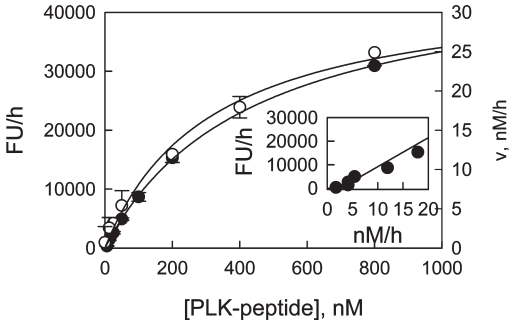

FIGURE 1: Comparison of two kinase assays. The LRRK2-catalyzed PLK-peptide phosphorylation was conducted under the same conditions as the TR-FRET assay and the radiometric assay. The initial velocities were measured as a function of PLK-peptide concentration at 200 μM ATP and 24 nM LRRK2. Filled circles correspond to the *y*-axis of FU/h on the left measured by the TR-FRET assay, while empty circles correspond to the *y*-axis of nM/h on the right determined from the radiometric assay. The data were fit to the simple Michaelis−Menten equation. Best fit parameters are as follows: $(k_{cat})_{app}$ = 31870 FU/h and $(K_{PLK})_{app}$ = 592 nM for the TR-FRET assay, and $(k_{cat})_{app}$ = 33.6 nM/h and $(K_{PLK})_{app}$ = 434 nM for the radiometric assay. The inset shows the linear correlation of the FU/h and nM/h units.

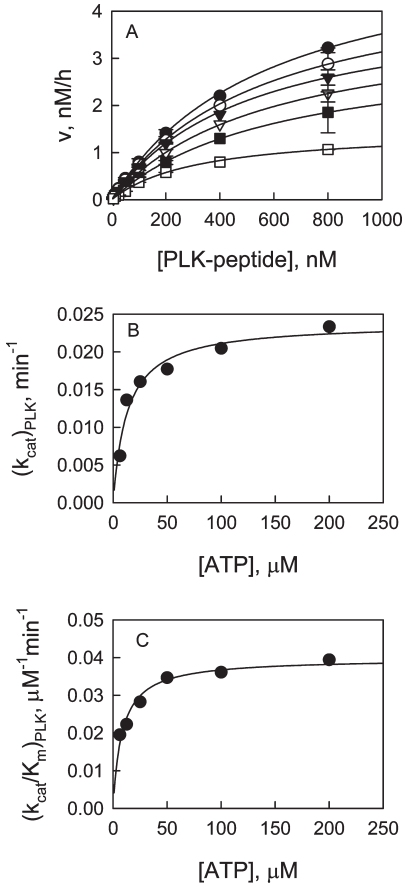

FIGURE 2: Steady-state kinetic studies of the LRRK2-catalyzed phosphorylation of PLK-peptide. (A) Dependence of initial velocities on PLK-peptide concentration at 200 (●), 100 (○), 50 (▼), 25 (▽), 12.5 (■), and 6.25 μM ATP (□). Each data point is the average of duplicate determinations. The data set was globally fit to the equation reflecting a rapid equilibrium random model. (B and C) ATP concentration dependencies of apparent $(k_{cat})_{PLK}$ and $(k_{cat}/K_m)_{PLK}$ values derived from analysis of the data in panel A.

To examine the data carefully and judge among the mechanisms, we also used the method of replots as described previously (*17*).

Table 1: Initial Velocity Analysis of LRRK2-Catalyzed Phosphorylation Reactions[a]

	PLK-peptide	LRRKtide
k_{cat} (min^{-1})	0.024 ± 0.002	0.10 ± 0.003
K_A (μM)	13 ± 2.9	67 ± 6.4
K_B (μM)	0.58 ± 0.08	29 ± 2.7
α	1.3 ± 0.2	1.1 ± 0.1

[a]The parameter estimates were calculated by globally fitting the data to the equation reflecting the rapid equilibrium random/steady-state order mechanism. Each parameter estimate is the average of two independent experiments. The error limit is the deviation from the mean. A represents ATP, and B represents a phosphoryl acceptor.

The starting point in this data analysis was to calculate apparent values of $(k_{cat})_X$ and $(k_{cat}/K_m)_X$ (X = PLK-peptide or ATP) by nonlinear least-squares fits of each individual plot of v_o versus [X] to the simple Michaelis−Menten equation. The next step in this analysis was to construct the replots of the dependencies of apparent values of $(k_{cat})_A$ and $(k_{cat}/K_m)_A$ on [B] and the dependencies of apparent values of $(k_{cat})_B$ and $(k_{cat}/K_m)_B$ on [A] and examine their shape. Replots will show a specific, mechanism-based pattern. For example, for the random mechanism of eq 3, apparent values of $(k_{cat})_A$ and $(k_{cat}/K_m)_A$ will be hyperbolically dependent on [B] according to eqs 4 and 5, respectively:

$$(k_{cat})_A = k_{cat}\left(\frac{[B]}{\alpha K_B + [B]}\right) \quad (4)$$

$$\left(\frac{k_{cat}}{K_m}\right)_A = \frac{k_{cat}}{\alpha K_A}\left(\frac{[B]}{K_B + [B]}\right) \quad (5)$$

Likewise, apparent values of $(k_{cat})_B$ and $(k_{cat}/K_m)_B$ will be hyperbolically dependent on [A].

Replots of apparent values of $(k_{cat})_{PLK}$ and $(k_{cat}/K_m)_{PLK}$ versus ATP concentration are hyperbolic (Figure 2B,C), and replots of apparent values of $(k_{cat})_{ATP}$ and $(k_{cat}/K_m)_{ATP}$ versus PLK concentration are hyperbolic as well (data not shown) and suggest that this reaction follows either a random or a steady-state ordered mechanism. Since the rate laws are mathematically equivalent for these mechanisms, they cannot be distinguished by the method of replots. However, they can be distinguished through the use of substrate analogue and product inhibition studies (see below).

Initial Velocity Studies of the LRRK2-Catalyzed Phosphorylation of LRRKtide. To determine the kinetic mechanism of the LRRK2-catalyzed phosphorylation of LRRKtide, initial velocities were measured over a range of concentrations of LRRKtide at several fixed concentrations of ATP (see the Supporting Information). The data set was globally fit to equations that reflect ping-pong, rapid equilibrium ordered, and random/steady-state ordered mechanisms. The random (or steady-state ordered) mechanism fits the data best and provides parameter estimates averaged from two independent experiments: k_{cat} = 0.1 ± 0.003 min^{-1}, K_{ATP} = 67 ± 6 μM, K_{PLK} = 29 ± 3 μM, and α = 1.1 ± 0.1 (summarized in Table 1). The analysis using the method of replots confirmed that this reaction follows either a random or a steady-state ordered mechanism.

Inhibition Studies for PLK-peptide Phosphorylation. To determine the kinetic mechanism of LRRK2-catalyzed PLK-peptide phosphorylation, an inhibition study was conducted with peptide substrate analogue LRRKtide^A, where threonine of LRRKtide was replaced with alanine, nucleotide analogues

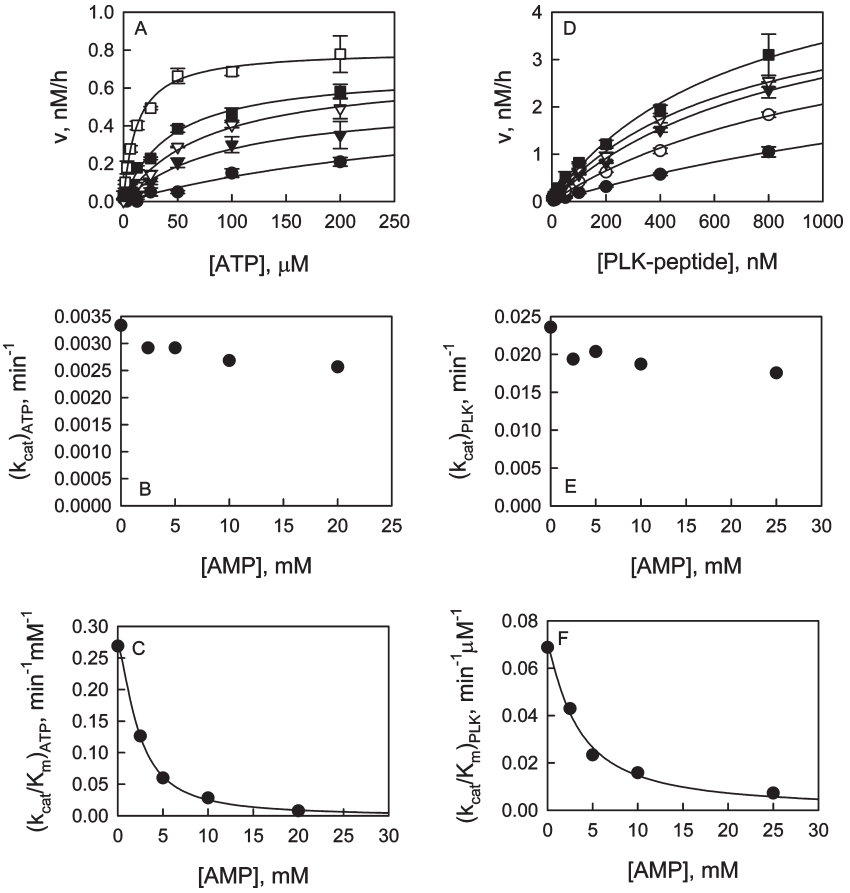

FIGURE 3: Inhibition study of the LRRK2-catalyzed phosphorylation of PLK-peptide by AMP. (A) Plot of initial velocities vs [ATP] at 25 (●), 10 (▼), 5 (▽), 2.5 (■), and 0 μM AMP (□), all at a fixed PLK-peptide concentration of 100 nM. (B and C) AMP concentration dependencies of apparent $(k_{cat})_{ATP}$ and $(k_{cat}/K_m)_{ATP}$ values derived from analysis of the data in panel A. (D) Plot of initial velocities vs [PLK-peptide] at 25 (●), 10 (○), 5 (▼), 2.5 (▽), and 0 mM AMP (■), all at a fixed ATP concentration of 200 μM. (E and F) AMP concentration dependencies of apparent $(k_{cat})_{PLK}$ and $(k_{cat}/K_m)_{PLK}$ values derived from analysis of the data in panel D.

AMP and AMP-PNP, and product ADP. Data were analyzed using methods of replots as described previously (*17*). As examples of this method, we analyzed inhibition by AMP. First, we determined (i) at a single [PLK-peptide], the dependence of v_0 on [ATP] at several concentrations of AMP (Figure 3A) and (ii) at a single [ATP], the dependence of v_0 on [PLK-peptide] at several concentrations of AMP (Figure 3D). Next, for (i), we analyzed the dependence of v_o on [ATP] at each [AMP] to calculate apparent values of $(k_{cat})_{ATP}$ and $(k_{cat}/K_m)_{ATP}$. For (ii), we analyzed the dependence of v_o on [PLK] at each [AMP] to calculate apparent values of $(k_{cat})_{PLK}$ and $(k_{cat}/K_m)_{PLK}$. Replots of apparent values of $(k_{cat})_X$ (X = ATP or PLK-peptide) versus [AMP] and apparent values of $(k_{cat}/K_m)_X$ versus [AMP] were then constructed, which will show a specific, mechanism-based pattern (*17*).

When ATP was the variable substrate, we found that apparent values of $(k_{cat})_{ATP}$ are independent of [AMP] (Figure 3B), but apparent values of $(k_{cat}/K_m)_{ATP}$ depend on [AMP] (Figure 3C) according to a simple inhibition expression of the general form $v_{inhib} = v_{control}/(1 + [I]/K_{i,app})$. This pattern indicates that AMP is competitive with ATP. More surprisingly, the same pattern was revealed when PLK-peptide was the variable substrate; apparent values of $(k_{cat})_{PLK}$ are independent of [AMP], but apparent values of $(k_{cat}/K_m)_{PLK}$ depend on [AMP] according to the equation $v_{inhib} = v_{control}/(1 + [I]/K_{i,app})$ (Figure 3E,F). Thus, AMP is competitive with PLK-peptide as well.

The inhibition study of peptide substrate analogue LRRKtide^A revealed that when PLK-peptide is the variable substrate, apparent values of $(k_{cat})_{PLK}$ are independent of [LRRKtide^A] but apparent values of $(k_{cat}/K_m)_{PLK}$ depend on [LRRKtide^A]; when ATP is the variable substrate, both apparent values of $(k_{cat})_{ATP}$ and $(k_{cat}/K_m)_{ATP}$ titrate with [LRRKtide^A] (see the Supporting Information). It suggests that LRRKtide^A is competitive with PLK-peptide but noncompetitive with ATP.

These patterns rule out a steady-state ordered mechanism but are different from the ones well-known for a random mechanism in which it has been assumed that the competitive inhibitors act as dead-end inhibitors and bind to the same enzyme form as the substrates (*18*). The patterns seen in this study clearly suggest that the inhibitors interact with the enzyme in a different mode. To examine these results and estimate values of inhibition constants, we used the method described in detail previously (*17*), where the general mechanism of Scheme 1 in which the inhibitor can bind to all four forms of the enzyme was used to derive the rate equation (eq 6) under rapid equilibrium conditions.

$$v = \frac{\dfrac{V_{max}[A]}{1+\dfrac{\alpha K_B}{[B]}+\dfrac{\alpha K_B}{[B]}\dfrac{[I]}{K_{i,ea}}+\dfrac{[I]}{K_{i,eab}}}}{K_A\left(\dfrac{\alpha+\dfrac{\alpha K_B}{[B]}+\dfrac{\alpha K_B}{[B]}\dfrac{[I]}{K_{i,e}}+\dfrac{[I]}{K_{i,eab}}}{1+\dfrac{\alpha K_B}{[B]}+\dfrac{\alpha K_B}{[B]}\dfrac{[I]}{K_{i,ea}}+\dfrac{[I]}{K_{i,eab}}}\right)+[A]} \quad (6)$$

By inspecting eqs 7−10 which describe the dependence of apparent values of $(V_{max})_X$ and $(V_{max}/K_m)_X$ (X = ATP or

Scheme 1: Rapid Equilibrium Random Mechanism of LRRK2-Catalyzed Phosphorylation[a]

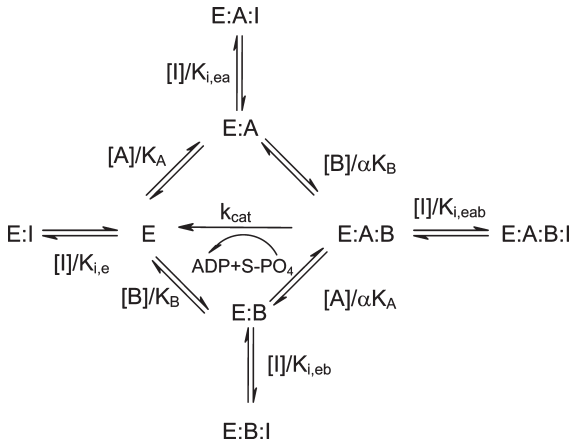

[a]A represents ATP, and B represents a phosphoryl acceptor, either PLK-peptide or LRRKtide.

PLK-peptide) on inhibitor, we can immediately see how inhibitors interact with the enzyme.

$$(V_{max})_{ATP} = \frac{V_{max}}{1 + \frac{\alpha K_B}{[B]} + \frac{\alpha K_B}{[B]}\frac{[I]}{K_{i,ea}} + \frac{[I]}{K_{i,eab}}} \quad (7)$$

$$(V_{max}/K_m)_{ATP} = \frac{V_{max}/\alpha K_A}{1 + \frac{K_B}{[B]} + \frac{K_B}{[B]}\frac{[I]}{K_{i,e}} + \frac{[I]}{K_{i,eb}}} \quad (8)$$

In the case of AMP inhibition where ATP is the variable substrate, apparent values of $(V_{max})_{ATP}$ are independent of [AMP], which suggests that both $K_{i,ea}$ and $K_{i,eab}$ are very large and AMP cannot bind to either the E·A complex or the E·A·B complex. On the other hand, apparent values of $(V_{max}/K_m)_{ATP}$ titrate with AMP, suggesting that AMP can bind E, the E·B complex, or both.

$$(V_{max})_{PLK} = \frac{V_{max}}{1 + \frac{\alpha K_A}{[A]} + \frac{\alpha K_A}{[A]}\frac{[I]}{K_{i,eb}} + \frac{[I]}{K_{i,eab}}} \quad (9)$$

$$(V_{max}/K_m)_{PLK} = \frac{V_{max}/\alpha K_B}{1 + \frac{K_A}{[A]} + \frac{K_A}{[A]}\frac{[I]}{K_{i,e}} + \frac{[I]}{\alpha K_{i,ea}}} \quad (10)$$

In the case where PLK-peptide is the variable substrate, apparent values of $(V_{max})_{PLK}$ are independent of [AMP], which means that both $K_{i,eb}$ and $K_{i,eab}$ are very large and clearly suggests that AMP cannot bind to the E·B complex. On the other hand, apparent values of $(V_{max}/K_m)_{PLK}$ titrate with AMP, suggesting that AMP can bind to E, and we can estimate $K_{i,e}$ directly from eq 10 with our previous knowledge of k_{cat}, K_A, K_B, and α.

Using this method, we also determined for nucleotide analogue AMP-PNP and product ADP the mechanism of inhibition and the inhibition dissociation constants (see the Supporting Information). All these data are summarized in Table 2.

Inhibition Studies of LRRKtide Phosphorylation. The kinetic mechanism of LRRK2-catalyzed LRRKtide phosphorylation was determined by conducting the inhibition studies with AMP, AMP-PNP, ADP, and peptide LRRKtide^A as well.

Table 2: Inhibition of LRRK2 Kinase by Substrate Analogues

inhibitor	substrate	mechanism	$K_{i,e}$ (mM)	$K_{i,ea}$ (mM)	$K_{i,eb}$ (mM)
AMP	ATP	C	2.2 ± 0.1		
	PLK-peptide	C	2.7 ± 0.5		
	ATP	C	2.2 ± 0.2		
	LRRKtide	NC	12 ± 0.2		14 ± 2.1
AMP-PNP	ATP	C	0.3 ± 0.03		
	PLK-peptide	NC	1.3 ± 0.3		2.3 ± 0.2
	ATP	C	0.7 ± 0.2		
	LRRKtide	NC	0.7 ± 0.1		1.8 ± 0.2
ADP	ATP	C	0.02 ± 0.003		
	PLK-peptide	NC	0.1 ± 0.03		0.3 ± 0.1
	ATP	C	0.2 ± 0.02		
	LRRKtide	NC	0.1 ± 0.01		0.2 ± 0.02
LRRKtide^A	ATP	NC	1.3 ± 0.4	0.65 ± 0.06	
	PLK-peptide	C		0.54 ± 0.05	
	ATP	NC	0.70 ± 0.20	0.90 ± 0.11	
	LRRKtide	C		0.54 ± 0.03	

When ATP is the variable substrate, AMP, AMP-PNP, and ADP are competitive with ATP while peptide substrate analogue LRRKtide^A is noncompetitive with ATP; when LRRKtide is the variable substrate, AMP, AMP-PNP, and ADP are noncompetitive with LRRKtide while LRRKtide^A is competitive with LRRKtide (see the Supporting Information). These inhibition patterns concur with a rapid equilibrium random mechanism with either ATP or LRRKtide being the first substrate to bind to the enzyme. Unlike the PLK-peptide phosphorylation, both AMP and LRRKtide^A behave as dead-end inhibitors and bind to both E and the E·X complex (X = ATP or LRRKtide). The inhibition dissociation constants were determined and are summarized in Table 2.

Steady-State Kinetic Study of LRRK2-Catalyzed Hydrolysis of GTP. To characterize LRRK2-catalyzed hydrolysis of GTP, we have developed a radiometric assay in which [α-^{33}P]GDP is separated from [α-^{33}P]GTP by TLC and counted by a scintillation counter. The production of GDP is linearly dependent on both time and enzyme concentration (data not shown). Initial velocities were measured as a function of GTP concentration. The dependence of initial velocity on GTP concentration adheres to the simple Michaelis−Menten equation, which allowed us to calculate the steady-state kinetic parameters by nonlinear least-squares fit (Figure 4) as summarized in Table 3: $k_{cat} = 0.23 \pm 0.02$ s^{-1}, and $K_m = 210 \pm 29$ μM. These results reveal that WT LRRK2 expressed in mouse brain has GTPase activity.

Solvent Isotope Effect Study of LRRK2-Catalyzed Hydrolysis of GTP. The initial velocities were measured in H_2O and D_2O (the molar fraction of D_2O equals 0.86) for k_{cat} at a saturating concentration of GTP (1 mM) at pH 7.4 and the pD equivalent (*19*), respectively. The solvent isotope effect ($^Dk_{cat} = 0.97 \pm 0.04$) is the mean of the ratio of k_{cat} in H_2O and D_2O from four independent experiments.

Inhibition Studies for GTP Hydrolysis. The inhibition studies of GTP hydrolysis were conducted with substrate analogues GMP and ADP and product GDP. The initial velocities were measured as a function of inhibitor concentration at 200 μM GTP. The dependence of the initial velocity on I (I = GMP, GDP, or ADP) adheres to the simple inhibition expression of the general form $v_{inhib} = v_{control}/(1 + [I]/K_{i,app})$, which allowed us to calculate apparent dissociation constants of 2.9 ± 0.3 mM, 97 ± 16 μM, and 0.6 ± 0.1 mM for GMP, GDP, and ADP, respectively (Figure 5). We converted the apparent dissociation

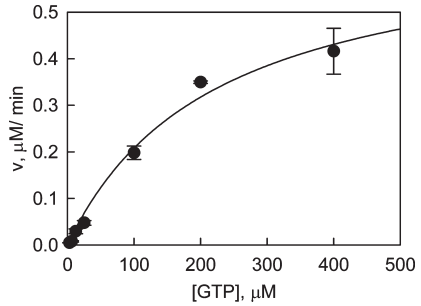

FIGURE 4: LRRK2-catalyzed GTP hydrolysis. The LRRK2-catalyzed GTP hydrolysis was conducted in buffer containing 20 mM Tris (pH 7.4), 50 mM NaCl, 10 mM $MgCl_2$, 1 mM DTT, 0.5 mg/mL BSA, GTP, and [α-^{33}P]GTP. The reaction was initiated by the addition of 30 nM LRRK2 and the mixture incubated at room temperature for 20 min. The reaction was stopped by the addition of 20 mM EDTA, and the product [α-^{33}P]GDP was separated from [α-^{33}P]GTP by PEI-cellulose TLC developed with 0.5 M KH_2PO_4 (pH 3.4) developing buffer and analyzed with a scintillation counter. Each data point is the average of triplicate determinations, and the error bars represent the standard deviation. The data set was fit to the simple Michaelis−Menten equation.

Table 3: Kinetic Constants of LRRK2-Catalyzed GTP Hydrolysis

k_{cat} (s^{-1})	K_{GTP} (μM)	$^{D}k_{cat}$
0.23 ± 0.02	210 ± 29	0.97 ± 0.04

constants into dissociation constants of 1.5 mM, 49 μM, and 0.3 mM for GMP, GDP, and ADP, respectively, by applying the Cheng−Prusoff equation for competitive inhibition as given in eq 11 (*20*).

$$K_{i,app} = K_i(1 + [S]/K_m) \quad (11)$$

Effects of Nucleotides on LRRK2-Catalyzed Phosphorylation. To determine the effects of nucleotides on the kinase activity of LRRK2, initial velocities of LRRK2-catalyzed phosphorylation of PLK-peptide were measured over a range of concentrations of nucleotides, GTP, GDP, and GMP, under conditions for k_{cat}, $(k_{cat}/K_m)_{ATP}$, and $(k_{cat}/K_m)_{PLK}$. No significant activation or inhibition of kinase activity was detected under any of the conditions. Figure 6 shows an example of the effect of a nucleotide on k_{cat} for the PLK-peptide phosphorylation. The effects of nucleotides on LRRK2-catalzyed phosphorylation of LRRKtide were also tested, and no significant activation or inhibition of kinase activity was detected (data not shown).

Effects of Kinase Activity on GTPase Activity. To determine the effects of kinase activity on the upstream GTPase activity of LRRK2, initial velocities of LRRK2-catalyzed GTP hydrolysis were measured in the presence of ADP, ATP, and PLK-peptide at 200 μM GTP. Inhibition of GTPase activity was detected in the presence of ADP or ATP, but not for PLK-peptide (Figure 7).

Inhibition of LRRK2 by Compound LDN-73794. We identified compound LDN-73794 through a screen of our compound collection of inhibitors of LRRK2 kinase activity with an IC_{50} of 3.5 ± 0.3 μM. To characterize this inhibitor, first we studied the mechanism of inhibition of LDN-73794 in the PLK-peptide phosphorylation. The studies were conducted in a manner identical to that outlined above for AMP. The primary plots of the dependence of v_0 on [ATP] and the dependence of v_0 on [PLK-peptide] were determined at several concentrations of

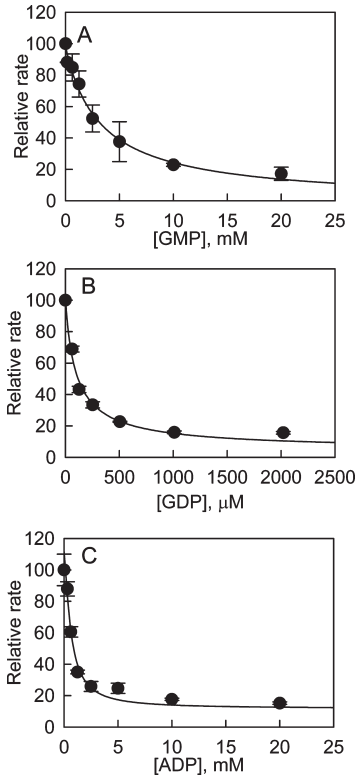

FIGURE 5: Inhibition of the LRRK2-catalyzed GTP hydrolysis by nucleotide analogues. The GTPase reaction was conducted at 200 μM GTP in the presence of GMP (A), GDP (B), or ADP (C). The dependence of relative rate on I (I = GMP, GDP, or ADP) was fit to the simple inhibition expression of the general form $v_{inhib} = v_{control}/(1 + [I]/K_{i,app})$, which allowed us to calculate apparent dissociation constants of 2.9 mM, 97 μM, and 0.6 mM for GMP, GDP, and ADP, respectively. Each data point is the average of triplicate determinations, and the error bars represent the standard deviation.

LDN-73794 (Figure 8). The replots of these data show that apparent values of $(k_{cat})_{ATP}$ are independent of the inhibitor and apparent values of $(k_{cat}/K_m)_{ATP}$ titrate with the inhibitor; both apparent values of $(k_{cat})_{PLK}$ and $(k_{cat}/K_m)_{PLK}$ titrate with the inhibitor. These patterns suggest that LDN-73794 is competitive with ATP and noncompetitive with PLK-peptide. By inspecting eqs 7−10 and using our previous knowledge of k_{cat}, K_A, K_B, and α, we estimate the inhibitor dissociation constants: $K_{i,e}$ = 2.0 ± 0.5 μM, and $K_{i,eb}$ = 3.1 ± 0.5 μM. Next we carried out the inhibition study for LDN-73794 in the GTPase assay. The initial velocity was measured as a function of LDN-73794 concentration at 200 μM GTP, and no inhibition was detected.

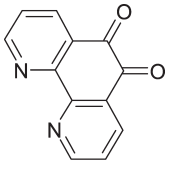

LDN-73794

DISCUSSION

LRRK2 is unusual in that it encodes two distinct but functionally linked enzymes: a protein kinase and a GTPase. Recent studies have suggested that LRRK2 is capable of undergoing both autophosphorylation and generic substrate phosphorylation, and the kinase activity is regulated by the GTPase domain (*8*−*12*). However, little is known about the kinetic mechanism of the two enzymatic properties. Our goal for these

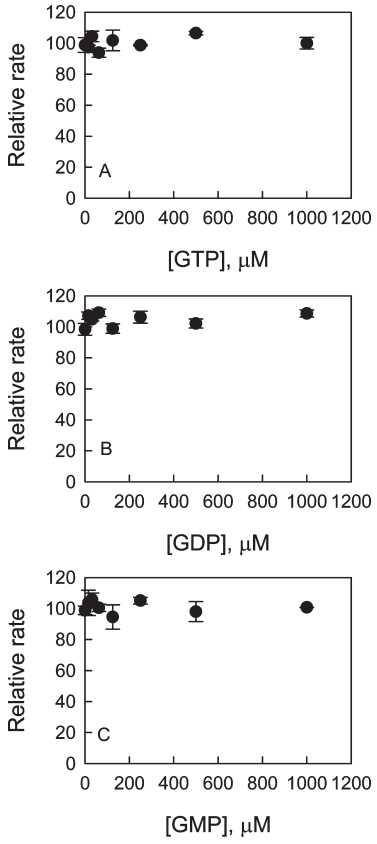

FIGURE 6: Effects of nucleotides on LRRK2-catalyzed PLK-peptide phosphorylation. The initial velocity of LRRK2-catalyzed phosphorylation of PLK-peptide was measured as a function of the concentration of GTP, GDP, or GMP at saturating concentrations of ATP and PLK. Each data point is the average of triplicate determinations, and the error bars represent the standard deviation.

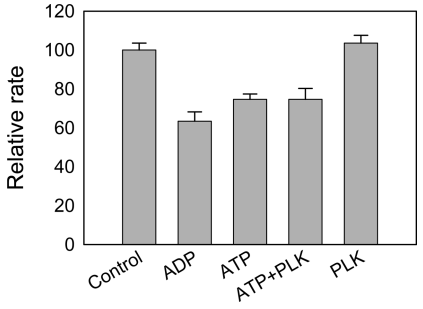

FIGURE 7: Inhibition of the LRRK2-catalyzed GTP hydrolysis. The GTPase reaction was conducted at 200 μM GTP in the presence of 0.5 mM ADP, 0.5 mM ATP, 0.5 mM ATP and 1 μM PLK, or 1 μM PLK. The control was conducted in the absence of either ADP/ATP or PLK. Each data point is the average of triplicate determinations, and the error bars represent the standard deviation.

studies was to understand the kinetic mechanism of LRRK2 that would be useful in designing a high-throughput screening assay and to establish a kinetic background for the interpretation of the mechanism of inhibition.

Kinetic Mechanism of the LRRK2 Kinase Property. There appears to be no consensus kinetic mechanism for protein kinases (*21*). In the majority of cases, protein kinases follow a random mechanism, while there are a number of examples of kinases following an ordered mechanism (*22*−*27*). In some cases, the nature of the substrate could influence the binding order as reported for p38α of the MAPK family: the kinetic mechanism of

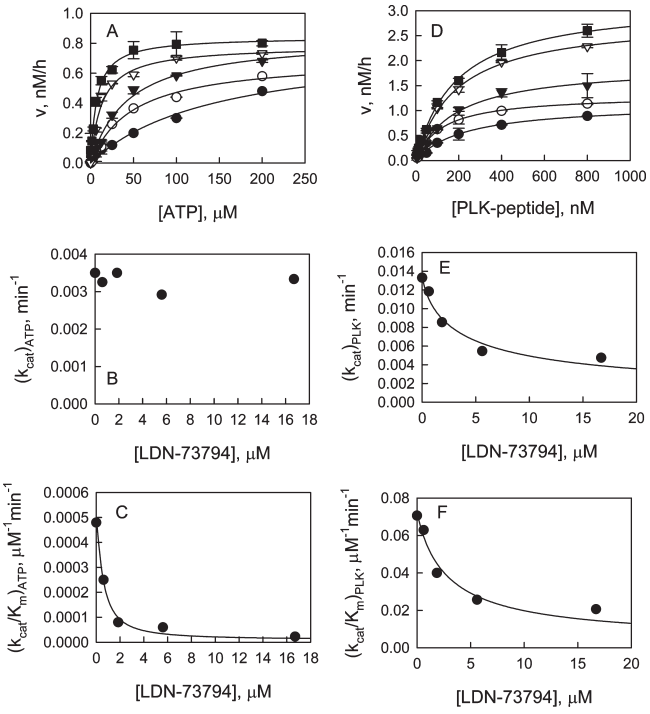

FIGURE 8: Inhibition of the LRRK2-catalyzed phosphorylation of PLK-peptide by compound LDN-73794. (A) Plot of initial velocities vs [ATP] at 16.7 (●), 5.6 (○), 1.85 (▼), 0.62 (▽), and 0 μM LDN-73794 (■), all at a fixed PLK-peptide concentration of 100 nM. (B and C) LDN-73794 concentration dependencies of apparent $(V_{max})_{ATP}$ and $(V_{max}/K_m)_{ATP}$ values derived from analysis of the data in panel A. (D) Plot of initial velocities vs [PLK-peptide] at 16.7 (●), 5.6 (○), 1.85 (▼), 0.62 (▽), and 0 μM LDN-73794 (■), all at a fixed ATP concentration of 50 μM. (E and F) LDN-73794 concentration dependencies of apparent $(V_{max})_{PLK}$ and $(V_{max}/K_m)_{PLK}$ values derived from analysis of the data in panel D.

p38α changes from one in which ATP binds to an enzyme before a peptide substrate (*28*) to one in which the protein ATF2 binds before ATP (*29*).

The physiological substrate of LRRK2 is still unclear, although recent studies reported that ezrine, radixin, and moesin (ERM), proteins that anchor the actin cytoskeleton to the plasma membrane, are efficiently phosphorylated by LRRK2 as potential substrates (*30*, *31*). A short peptide substrate, LRRKtide, that encompasses Thr^{558} of moesin (RLGRDKYKTLRQIRQ) has been widely used in the characterization of LRRK2 catalysis, but the kinetic mechanism of the reaction has not been reported. In our studies of this enzyme, we sought to probe the kinetic mechanism with two peptide substrates, LRRKtide and PLK-peptide derived from PLK protein, and to determine whether a common kinetic mechanism is shared by these two phosphoryl acceptors. Our initial velocity data with both PLK-peptide and LRRKtide suggest a random or steady-state ordered mechanism. To distinguish between these two mechanisms, we conducted substrate analogue and product inhibition studies (*16*, *18*, *32*). The results of these studies are summarized in Table 2. For LRRK2-catalyzed phosphorylation of PLK-peptide, we found that nucleotide analogue AMP is competitive with both ATP and PLK-peptide; substrate analogue $LRRKtide^A$ is competitive with PLK-peptide and noncompetitive with ATP. Different patterns were seen with LRRKtide as the phosphoryl acceptor. AMP is competitive with ATP and noncompetitive with LRRKtide; substrate analogue $LRRKtide^A$ is competitive with LRRKtide and noncompetitive with ATP. To elucidate the

kinetic mechanism, we also tested nucleotide analogue AMP-PNP and product ADP in the two reactions and found AMP-PNP and ADP are competitive with ATP in both reactions and noncompetitive with the phosphoryl acceptors, PLK-peptide and LRRKtide. The substrate analogue and product inhibition patterns rule out a steady-state ordered mechanism and indicate a rapid equilibrium random mechanism for phosphorylation of both PLK-peptide and LRRKtide (*18*, *32*). The nature of the peptide substrate does not influence the substrate binding order with LRRK2, although the binding of PLK-peptide induces a conformation change that prohibits AMP from binding. In both reactions, either ATP or phosphoryl acceptor (PLK-peptide or LRRKtide) can bind to the enzyme first to form the enzyme·substrate binary complex followed by the formation of the ternary complex. The equilibrium of these species shown in Scheme 1 was attained prior to the rate-limiting step, which may be the chemistry step, or some steps following the chemistry step. The binding of the first substrate does not affect the binding affinity of the second substrate as demonstrated by the cofactor α with a value close to 1.

Formation of a Nonproductive Complex. Unexpectedly, values of K_{ATP} for the reaction of LRRK2 with PLK-peptide and LRRKtide depend on the identity of the phosphoryl acceptor, equaling 13 and 67 μM, respectively. Values of $K_{i,e}$ for AMP also differ 5-fold in the two reactions, equaling 2.5 and 12 μM for PLK-peptide and LRRKtide, respectively. K_{ATP} and $K_{i,e}$ are dissociation constants, and their magnitudes are supposed to be identical regardless of the identity of the phosphoryl acceptor. A mechanism that involves the formation of a nonproductive binary complex upon the binding of the phosphoryl acceptor to free enzyme, to which nucleotides bind nonproductively, could account for these results. Thus, the measured values are complex terms that include the contribution from the pathway introduced by the nonproductive binding of the phosphoryl acceptor and would be dependent on the identity of the phosphoryl acceptor.

Characterization of the GTPase Activity of LRRK2. It has been reported that LRRK2 possesses a GTPase activity (*10*, *15*). Here we characterize LRRK2-catalyzed GTP hydrolysis. The production of GDP is linearly dependent on both time and enzyme concentration. The dependence of the initial velocity of GDP production on GTP concentration adheres to the simple Michaelis−Menten equation and allowed us to calculate the steady-state kinetic parameters. No solvent kinetic isotope effect could be detected on k_{cat}, which suggests that the rate-limiting step of the reaction governed by k_{cat} is the release of product GDP. In other words, the product release step is slower than the chemical step. That was not surprising, since like all the other G-proteins, the GTP binding domain of LRRK2 undergoes a switch cycle between the GTP-bound active and GDP-bound inactive forms. The exchange of GDP for GTP is promoted by either guanine nucleotide exchange factors (GEFs) or a dimerization-induced conformation change.

Relationship of Kinase and GTPase Activities. It has been reported that the kinase activity of LRRK2 is regulated by the GTPase domain such that the binding of GTP stimulates LRRK2 kinase activity (*8*, *10*, *11*). To understand the functional regulation between the kinase and GTPase activity, we first tested the effect of nucleotides (GTP, GDP, and GMP) in a dose−response manner on LRRK2-catalyzed PLK-peptide phosphorylation under conditions for k_{cat} and k_{cat}/K_m. No significant activation or inhibition of kinase activity in the presence of nucleotides was detected under the condition that was tested. To exclude the possibility that our results are substrate-dependent, we also conducted the same studies for LRRK2-catalyzed LRRKtide phosphorylation, and no significant effect was detected. It might be possible that we missed the GTP activation given the fact that the reaction progress curve for GTPase reaction was linear only up to 30 min and we typically incubate the kinase reaction mixture for at least 2 h. Therefore, the effect of nucleotide binding on kinase activity was tested as a time course, but no significant effect could be detected. The lack of GTPase domain regulation on kinase activity might suggest that the brain LRRK2 that was used in this study is already in a nucleotide-bound state, either a GTP- or GDP-bound state. We hypothesized that it was likely in the inactive GDP-bound state, since the product GDP release step is slow compared with the chemical step as suggested by the SKIE study. To test this hypothesis, we examined the effect of product GDP and nucleotide analogue GMP on the GTPase activity and found that both GDP and GMP inhibit the GTPase activity of LRRK2. The lack of an effect of the nucleotides on kinase activity makes the hypothesis that GTP binding stimulates LRRK2 kinase activity controversial. A previous study demonstrated that the nonhydrolyzable GTP analogue, GPP(NH)p, but not GTP, increased LRRK2 kinase activity, whereas GDP had no effect on kinase activity instead of inhibiting kinase activity as predicted (*10*). It is important to note that the effect seen here is based on in vitro assays performed on two generic substrates. There are some cellular GTPase regulators under physiological conditions, such as GTPase-activating proteins (GAP), that have been shown to stimulate GTP hydrolysis which in turn could regulate kinase activity.

To improve our understanding of the functional relationship between the kinase and GTPase activity of LRRK2, i.e., the effect of the downstream kinase activity on GTPase activity, we also tested the effects of substrates or the product of the kinase reaction, such as ATP, PLK-peptide, or ADP, on the GTPase activity. We found that ADP and ATP, but not PLK-peptide, could inhibit the GTPase activity. There are two possibilities in which ADP or ATP could inhibit GTPase activity. (i) ADP or ATP binds directly to the active site of the GTPase domain, or (ii) ADP or ATP binds to the kinase domain and induces a conformational change that affects the GTPase activity. The second mechanism is not likely, though, given the fact that a nonspecific kinase inhibitor, staurosporine, inhibits LRRK2 kinase activity but does not inhibit GTPase activity at all (data not shown). To understand how ADP inhibits the GTPase activity, the dissociation constant of ADP was determined for both reactions: K_i = 20 μM in the kinase reaction, and K_i = 0.6 mM in the GTPase reaction. The 30-fold difference in dissociation constants of ADP suggests that there might be two distinct binding sites of ADP on LRRK2, and ADP could bind directly to the GTPase domain and inhibit GTPase activity.

Mechanism of Inhibition of LDN-73794. With knowledge of the kinetic mechanism of LRRK2-catalyzed phosphorylation, we were able to conduct a kinetic analysis of inhibitor LDN-73794 identified through a screen to understand the mechanism of inhibition, to estimate its inhibition constants, and to test its effect on the GTPase activity (Table 4). Studies of inhibition by LDN-73794 revealed that this compound is a well-behaved inhibitor with no hint of time dependence or partial inhibition. The dependence of initial velocity on inhibitor concentration can be described by the simple inhibition expression of the general form $v_{inhib} = v_{control}/(1 + [I]/K_{i,app})$ with no need to include the higher-order terms to attain good data fitting. As a result of a previous screen of cyclin-dependent kinase5 inhibitors (cdk5),

Table 4: Inhibition of LRRK2 Kinase by Compound LDN-73794

inhibitor	substrate	mechanism	$K_{i,e}$ (μM)	$K_{i,eb}$ (μM)
LDN-73794	ATP	C	1.2 ± 0.3	
	PLK-peptide	NC	2.0 ± 0.5	3.1 ± 0.5

LDN-73794 did not inhibit cdk5. It is unlikely that LDN-73794 shows inhibition by chelation of magnesium, since cdk5 kinase also requires Mg^{2+} for the catalytic activity. The studies of the mechanism of inhibition revealed that LDN-73794 is a competitive inhibitor of the binding of ATP and a noncompetitive inhibitor of PLK-peptide. It inhibits the kinase activity but has no effect on the GTPase activity. Further characterization of the mechanisms by which LDN-73794 interacts with WT LRRK2 and mutant LRRK2 is underway.

These studies establish a background of kinetic data that is essential in designing a high-throughput screening assay that allows identification of inhibitors interacting directly with the kinase domain and also allosteric inhibitors that modulate kinase activity through interaction with other LRRK2 domains. Identification of molecules that inhibit LRRK2's kinase activity not only can become the starting point for drug development for the treatment of PD but also can provide useful probes for further investigating the physiological functions of LRRK2 in normal cellular biology and in pathological conditions.

SUPPORTING INFORMATION AVAILABLE

Data from inhibition studies of AMP, AMP-PNP, and ADP for PLK-peptide and LRRKtide phosphorylation. This material is available free of charge via the Internet at http://pubs.acs.org.

REFERENCES

1. Moore, D. J., West, A. B., Dawson, V. L., and Dawson, T. M. (2005) Molecular pathophysiology of Parkinson's disease. *Annu. Rev. Neurosci. 28*, 57–87.
2. Paisán-Ruíz, C., Jain, S., Evans, E. W., Gilks, W. P., Simón, J., van der Brug, M., López de Munain, A., Aparicio, S., Gil, A. M., Khan, N., Johnson, J., Martinez, J. R., Nicholl, D., Carrera, I. M., Pena, A. S., de Silva, R., Lees, A., Martí-Massó, J. F., Pérez-Tur, J., Wood, N. W., and Singleton, A. B. (2004) Cloning of the gene containing mutations that cause PARK8-linked Parkinson's disease. *Neuron 44*, 595–600.
3. Zimprich, A., Biskup, S., Leitner, P., Lichtner, P., Farrer, M., Lincoln, S., Kachergus, J., Hulihan, M., Uitti, R. J., Calne, D. B., Stoessl, A. J., Pfeiffer, R. F., Patenge, N., Carbajal, I. C., Vieregge, P., Asmus, F., Müller-Myhsok, B., Dickson, D. W., Meitinger, T., Strom, T. M., Wszolek, Z. K., and Gasser, T. (2004) Mutations in LRRK2 cause autosomal-dominant parkinsonism with pleomorphic pathology. *Neuron 44*, 601–607.
4. Berg, D., Schweitzer, K., Leitner, P., Zimprich, A., Lichtner, P., Belcredi, P., Brussel, T., Schulte, C., Maass, S., and Nagele, T. (2005) Type and frequency of mutations in the LRRK2 gene in familial and sporadic Parkinson's disease. *Brain 128*, 3000–3011.
5. Khan, N. L., Jain, S., Lynch, J. M., Pavese, N., Abou-Sleiman, P., Holton, J. L., Healy, D. G., Gilks, W. P., Sweeney, M. G., Ganguly, M., Gibbons, V., Gandhi, S., Vaughan, J., Eunson, L. H., Katzenschlager, R., Gayton, J., Lennox, G., Revesz, T., Nicholl, D., Bhatia, K. P., Quinn, N., Brooks, D., Lees, A. J., Davis, M. B., Piccini, P., Singleton, A. B., and Wood, N. W. (2005) Mutations in the gene LRRK2 encoding dardarin (PARK8) cause familial Parkinson's disease: Clinical, pathological, olfactory and functional imaging and genetic data. *Brain 128*, 2786–2796.
6. Mata, I. F., Kachergus, J. M., Taylor, J. P., Lincoln, S., Aasly, J., Lynch, T., Hulihan, M. M., Cobb, S. A., Wu, R. M., Lu, C. S., Lahoz, C., Wszolek, Z. K., and Farrer, M. J. (2005) Lrrk2 pathogenic substitutions in Parkinson's disease. *Neurogenetics 6*, 171–177.
7. Paisán-Ruíz, C., Jain, S., Evans, E. W., Gilks, W. P., Simón, J., van der Brug, M., López de Munain, A., Aparicio, S., Gil, A. M., Khan, N., Johnson, J., Martinez, J. R., Nicholl, D., Carrera, I. M., Pena, A. S., de Silva, R., Lees, A., Martí-Massó, J. F., Pérez-Tur, J., Wood, N. W., and Singleton, A. B. (2004) Cloning of the gene containing mutations that cause PARK8-linked Parkinson's. *Neuron 44*, 595–600.
8. Smith, W. W., Pei, Z., Jiang, H., Dawson, V. L., Dawson, T. M., and Ross, C. A. (2006) Kinase activity of mutant LRRK2 mediates neuronal toxicity. *Nat. Neurosci. 9*, 1231–1233.
9. Greggio, E., Zambrano, I., Kaganovich, A., Beilina, A., Taymans, J. M., Daniëls, V., Lewis, P., Jain, S., Ding, J., Syed, A., Thomas, K. J., Baekelandt, V., and Cookson, M. R. (2008) The Parkinson disease-associated leucine-rich repeat kinase 2 (LRRK2) is a dimer that undergoes intramolecular autophosphorylation. *J. Biol. Chem. 283*, 16906–16914.
10. Guo, L., Gandhi, P. N., Wang, W., Petersen, R. B., Wilson-Delfosse, A. L., and Chen, S. G. (2007) The Parkinson's disease-associated protein, leucine-rich repeat kinase 2 (LRRK2), is an authentic GTPase that stimulates kinase activity. *Exp. Cell Res. 313*, 3658–3670.
11. Ito, G., Okai, T., Fujino, G., Takeda, K., Ichijo, H., Katada, T., and Iwatsubo, T. (2007) GTP binding is essential to the protein kinase activity of LRRK2, a causative gene product for familial parkinsons's disease. *Biochemistry 46*, 1380–1388.
12. West, A. B., Moore, D. J., Biskup, S., Bugayenko, A., Smith, W. W., Ross, C. A., Dawson, V. L., and Dawson, T. M. (2005) Parkinson's disease-associated mutations in leucine-rich repeat kinase 2 augment kinase activity. *Proc. Natl. Acad. Sci. U.S.A. 102*, 16842–16847.
13. Smith, W. W., Pei., Z., Jiang, H., Moore, D. J., Liang, Y., West, A. B., Dawson, V. L., Dawson, T. M., and Ross, C. A. (2005) Leucine-rich repeat kinase 2 (LRRK2) interacts with parkin, and mutant LRRK2 induces neuronal degeneration. *Proc. Natl. Acad. Sci. U.S.A. 102*, 18676–18681.
14. Greggio, E., Jain, S., Kingsbury, A., Bandopadhyay, R., Lewis, P., Kaganovich, A., van der Brug, M. P., Beilina, A., Blackinton, J., Thomas, K. J., Ahmad, R., Miller, D. W., Kesavapany, S., Singleton, A., Lees, A., Harvey, R. J., Harvey, K., and Cookson, M. R. (2006) Kinase activity is required for the toxic effects of mutant LRRK2/dardarin. *Neurobiol. Dis. 23*, 329–341.
15. Li, X., Tan, Y. C., Poulose, S., Olanow, C. W., Huang, X. Y., and Yue, Z. (2007) Leucine-rich repeat kinase 2 (LRRK2)/PARK8 possesses GTPase activity that is altered in familial Parkinson's disease R1441C/G mutants. *J. Neurochem. 103*, 238–247.
16. Segel, I. H. (1975) Enzyme Kinetics, John Wiley & Sons, New York.
17. Liu, M., Choi, S., Cuny, G. D., Ding, K., Dobson, B. C., Glicksman, M. A., Auerbach, K., and Stein, R. L. (2008) Kinetic studies of Cdk5/p25 kinase: Phosphorylation of tau and complex inhibition by two prototype inhibitors. *Biochemistry 47*, 8367–8377.
18. Fromm, H. J. (1979) Use of competitive inhibitors to study substrate binding order. *Methods Enzymol. 63*, 467–486.
19. Quinn, D. M., and Sutton, L. D. (1991) in Enzyme Mechanism from Isotope Effects (Cook, P. F., Ed.) pp 73−126, CRC Press, Boston.
20. Cheng, Y. C., and PRusoff, W. H. (1973) Relationship between the inhibition constant (K_1) and the concentration of inhibitor which causes 50% inhibition (I_{50}) of an enzymatic reaction. *Biochem. Pharmacol. 22*, 3099–3108.
21. Adams, J. A. (2001) Kinetic and catalytic mechanisms of protein kinases. *Chem. Rev. 101*, 2271–2290.
22. Songyang, Z., Lu, K. P., Kwon, Y. T., Tsai, L. H., Filhol, O., Cochet, C., Brickey, D. A., Soderling, T. R., Bartleson, C., Graves, D. J., DeMaggio, A. J., Hoekstra, M. F., Blenis, J., Hunter, T., and Cantley, L. C. (1996) A structural basis for substrate specificities of protein Ser/Thr kinases: Primary sequence preference of casein kinases I and II, NIMA, phosphorylase kinase, calmodulin-dependent kinase II, CDK5, and Erk1. *Mol. Biol. Cell 16*, 6486–6493.
23. Tabatabai, L. B., and Graves, D. J. (1978) Kinetic mechanism and specificity of the phosphorylase kinase reaction. *J. Biol. Chem. 253*, 2196–2202.
24. Walker, D. H., Kuppuswamy, D., Visvanathan, A., and Pike, L. J. (1987) Substrate specificity and kinetic mechanism of human placental insulin receptor/kinase. *Biochemistry 26*, 1428–1433.
25. Boerner, R. J., Barker, S. C., and Knight, W. B. (1995) Kinetic mechanisms of the forward and reverse pp60c-src tyrosine kinase reactions. *Biochemistry 34*, 16419–16423.
26. Cole, P. A., Grace, M. R., Phillips, R. S., Burn, P., and Walsh, C. T. (1995) The role of the catalytic base in the protein tyrosine kinase Csk. *J. Biol. Chem. 270*, 22105–22108.
27. Cole, P. A., Burn, P., Takacs, B., and Walsh, C. T. (1994) Evaluation of the catalytic mechanism of recombinant human Csk (C-terminal Src kinase) using nucleotide analogs and viscosity effects. *J. Biol. Chem. 269*, 30880–30887.

28. Chen, G., Porter, M. D., Bristol, J. R., Fitzgibbon, M. J., and Pazhanisamy, S. (2000) Kinetic mechanism of the p38-α MAP kinase: Phosphoryl transfer to synthetic peptides. *Biochemistry 39*, 2079–2087.
29. LoGrasso, P. V., Frantz, B., Rolando, A. M., O'Keefe, S. J., Hermes, J. D., and O'Neill, E. A. (1997) Kinetic mechanism for p38 MAP kinase. *Biochemistry 36*, 10422–10427.
30. Jaleel, M., Nichols, R. J., Deak, M., Campbell, D. G., Gillardon, F., Knebel, A., and Alessi, D. R. (2007) LRRK2 phosphorylates moesin at threonine-558: Characterization of how Parkinson's disease mutants affect kinase activity. *Biochem. J. 405*, 307–317.
31. Parisiadou, L., Xie, C., Cho, H. J., Lin, X., Gu, X. L., Long, C. X., Lobbestael, E., Baekelandt, V., Taymans, J. M., Sun, L., and Cai, H. (2009) Phosphorylation of ezrin/radixin/moesin proteins by LRRK2 promotes the rearrangement of actin cytoskeleton in neuronal morphogenesis. *J. Neurosci. 29*, 13971–13980.
32. Rudolph, F. B. (1979) Product inhibition and abortive complex formation. *Methods Enzymol. 63*, 411–436.